ORIGINAL SCIENTIFIC PAPER

CROATICA CHEMICA ACTA

Croat. Chem. Acta **2024**, *97*(3), 103–118
Published online: November 20, 2024
DOI: 10.5562/cca4110

HKD 1926

General Recursion Equations for Determining the Characteristic and Matching Polynomials of Benzenoid and Related Series and Analytical Expressions for Determining the Number of Dewar Resonance Structures

Jerry Ray Dias

Department of Chemistry, University of Missouri, Kansas City, MO 64110-2499, USA
* Author's e-mail address: diasj@umkc.edu

RECEIVED: July 13, 2024 * REVISED: October 28, 2024 * ACCEPTED: November 4, 2024

Abstract: Basic characteristic and matching polynomials for benzenoid series are given. Their recursion equations allow one to obtain the characteristic and matching polynomials and the number Dewar Resonance Structures (*DSs*) of very large members not accessible by other means. It is shown that conjugation is a stronger stabilizing effect than aromaticity. The success of topological resonance energy (TRE) as an index of aromatic stabilization energy (ASE) is because changes in conjugation energy (CE) occur in parallel with changes in aromatic stabilization energy. In the absence of ASE, CE becomes decisive.

Keywords: benzenoid hydrocarbons, aromatic resonance stabilization, conjugation energy, Dewar resonance structures, topological resonance energy, recursion equations.

INTRODUCTION

THE characteristic and matching polynomials provide a powerful molecular orbital based indices for studying π–electronic trends in homologous series of conjugated polyene hydrocarbons. The advantage to studying homologous series is that for the discerned trends, one can use known properties of a few lower members and reliably predict unknown properties for higher members. This is made possible because at the HMO level, analytical and recursion equations can be derived for these homologous series. Frequent themes include relative aromaticity, bandgaps, conjugation, magnetotropiciy, stability, and reactivity in regard to their observed and predicted chemical and physical properties. The matching polynomial (also, called acyclic polynomial) has been useful in determining topological resonance energy (TRE)[1,2] and the number of Dewar resonance structures (*DSs*)[3–5] of polycyclic conjugated hydrocarbons (PCHs). While the coefficients of characteristic polynomial can be computed by summing all the Sachs graphs, the coefficients of the matching polynomial are computed by summing all the Sachs without cyclic components. The matching polynomial is a characteristic polynomial of the hypothetical acyclic reference structure devoid of cyclic contributions against which the characteristic polynomial of a cyclic/polycyclic structure can be compared for purposes of determining resonance energy. Thus, TRE represents stabilization energy solely due to cyclic π–contributions because the π–binding energy determined by the matching polynomial of the hypothetical polyene reference is devoid of cyclic contributions. Both the actual molecule and its hypothetical polyene reference molecule have the same graph theoretical weights of their edges and vertices. Thus, they have the same geometry, electronic configuration, atomic hybridization, number of π-electrons, and same degree of steric strain.[6]

The characteristic and matching polynomials for acyclic conjugated polyenes are identical whereas for cyclic/polycyclic systems they are different. The matching polynomial does not include cyclic contributions, only adjacent conjugation interactions (so called dimer covering), whereas the characteristic polynomial includes both kinds of contributions. Thus, the matching polynomial can also be used to determine a HMO-like energy [E_π(ref)] for the hypothetical polyene reference molecule which when subtracted from the HMO total π energy (E_π) of a PAH molecule will give its topological resonance energy [TRE = E_π – E_π(ref)] which emanates principally from its cyclic contributions.[1,2] The TRE of different PAH molecules can be compared via their percentage TRE (%TRE) which is 100 times TRE divided by total binding energy [E_π(ref)] of the polyene reference. Aihara's %TRE is used as a measure of global aromaticity normalized with respect to the molecular size. The hypothetical polyene reference molecule above can be used to obtain a hypothetical HOMO-LUMO gap which when divided into the HOMO-LUMO gap of the actual molecule gives a quantity used as an index of kinetic stability called reduced HOMO-LUMO gap; in general, reduced HOMO-LUMO gaps < 1.30 are very reactive molecules.[7] Using benzene as an example, TRE = E_π(characteristic polynomial for benzene) – E_π(matching polynomial for benzene) = E_π(benzene) – E_π(ref) = 8.0000 – 7.7274 = 0.2726 β, %TRE = (0.2726 / 7.7274) × 100 = 3.53. The ΔE_π(benzene) = HOMO-LUMO gap = 2.0 β for the benzene and for its reference ΔE_π(ref) = HOMO-LUMO reference gap = 1.0353 β. The reduced HOMO-LUMO gap = 2.0000 / 1.0353 = 1.9318. All total resonant sextet benzenoids (benzenoids having their number of carbons divisible by 6, are totally covered by disjoint Clar sextets, and have number of bay regions given by $\eta_o(\max) = \frac{1}{2}N_H - 3$)[8] have reduced HOMO-LUMO gaps > 1.932.

The resonance energy of a benzenoid is the sum of aromatic stabilization energy (ASE) and conjugation energy (CE). Since TRE is an index measuring ASE, E_π(ref) determined from the matching polynomial minus the number of isolated ethene pπ-bonds is an index measuring topological conjugation energy (TCE). Hückel resonance energy (HRE) is then given by

$$\text{HRE} = \text{TRE} + \text{TCE}$$

Benzene for example has TRE = 0.2726 β and TCE = 7.7274 β – 6.0 β = 1.7274 β and HRE = 0.2726 β + 1.7274 β = 2.0 β. Thus, at the HMO level, TCE is larger than TRE. At the BLW-B3LYP/pVTZ level of theory, ASE = 25.7 kcal/mol, CE = 3 × 12.7 = 38. 1 kcal/mol, and RE = 65.4, i.e., ASE + CE = 63.8 kcal/mol which compares favorably with RE = 65.4 kcal/mol.(Table 7. in ref.; also see Scheme 2).[9] Again, CE is larger than ASE for benzene at the BLW-B3LYP/pVTZ level of theory. Given the large success using TRE for measuring relative ASE, we will employ TCE as an index for measuring relative CE. What Eq (1) further shows is that both TRE and TCE change proportionally. This explains why TRE is so successful as an index for ASE and why CE does not need to be explicitly considered at the HMO level of theory.

Both the linear polyacene series and the zigzag polyphenacene series have been extensively studied, separately,[10–17] comparatively,[18–21] and included within a broader context.[7,22–26] Quinododimethide analog series of linear polyacene and zigzag polyphenacene series have been the subject several studies.[5,27,28] The aromaticity and magnetotropicity of linear dicyclopenta-fused polyacenes have been analyzed.[29] The %TRE is defined as 100 times the TRE divided by the total binding energy of the polyene reference. TRE is an extensive property (naturally increases as molecular size increases) and %TRE is an intensive property.[6] Thus, the latter is used when comparing polycyclic aromatic molecules of different sizes. TRE and %TRE are standard measures of aromatic stabilization energy (ASE) and the reduced HOMO-LUMO gap is a measure of reactivity of the molecule.[1,7,29]

The classical Kekulé-structure-based model works well for small to medium sized conjugated systems not having essentially single bonds. For small to medium sized conjugated systems the classical Kekulé-structure-based model works well because Kekulé structures dominate over Dewar structures which are only 3 % as important.[3] Methods for enumerating Kekulé structures are both easier and well-known compared to methods for enumerating Dewar resonance structures. But as the benzenoid system gets larger, the number of Dewar structures escalates much faster than does the number of Kekulé structures. The consequence of this is that for small conjugated systems Kekulé resonance structures dominate but as the conjugated system get larger, Dewar resonance structures become more dominant by their sheer numbers. As two extreme examples, linear polyenes ($C_{2n}H_{2n+2}$) all have $\boldsymbol{K} = 1$ but $DS = \frac{1}{2}[n^2 - n]$ and monocyclic polyenes ($C_{2n}H_{2n}$) all have $\boldsymbol{K} = 2$ but $DS = [n^2 - 2n]$ where n = number of conjugated double bonds. The coefficients of both the characteristic and matching polynomials contain information on Kekulé and Dewar resonance structures.

Differences Between the Characteristic and Matching Polynomials and Their Corresponding Graphs

All the characteristic and matching polynomials in this study were obtained by using the programs of Balasubramanian.[30,31] Because the matching polynomial is devoid of cyclic contributions, it has no odd terms and if zero eigenvalue occurs in plus/minus pairs, i.e., the pairing theorem[32] applies to matching polynomial for even carbon nonAHs as well for AHs molecular graphs whereas for the

characteristic polynomial the pairing theorem only applies to AH molecular graphs. In addition, the matching polynomial of all odd carbon monocyclic molecular graphs have a one zero eigenvalue with otherwise paired eigenvalues. Another difference between the characteristic polynomial and the matching polynomial is for molecular graphs having greater than two-fold symmetry, two-thirds of the eigenvalues are doubly degenerate for the characteristic polynomial but not for the matching polynomial. [21,33,34] The same lack of degeneracy will be evident from the matching eigenvalues for benzene with $\boldsymbol{D}_{6v}$ symmetry. The first two coefficients to both the characteristic and matching polynomials of any given molecular graph are identical (namely, $a_0 = 1$, $a_2 = -q$ = No. edges). In addition, our original derivation of a_4 and a_6 can be used except the cyclic parameters will need to be omitted for the matching polynomial. They are $a_4^{ac} = (1/2)(q^2 - 9q + 6N_c) - d_1 - d_4 - 3d_5 - 6d_6 - \ldots$ and $a_6^{ac} = -(1/6)(q^3 - 27q + 116q) - N_c(3q - 16) - e(3,3) + (q - 6)e(2,1) + (q - 5)e(3,1)$ where N_c = number of carbon vertices, d_i = number of vertices of degree-i, and $e(j,k)$ = number of edges between vertices of degree-j and degree-k; note that a_4^{ac} is applicable to all graphs whereas a_6^{ac} is applicable to all molecular graphs of degree-3 or less. The absolute value of the tail coefficient ($|a_N^{ac}| = \boldsymbol{K}$) is equal to the number of Kekulé structures, if any, and $a_{N-2}^{ac} = (N_c/2)\boldsymbol{K} + DS$ where DS is the number of Dewar structures. Since the coefficients of the characteristic polynomial is the sum ($a_j = a_j^c + a_j^{ac}$) of the cyclic (a_j^c) and acyclic (a_j^{ac}) components with the latter given by the matching polynomial if one knows the characteristic polynomial value of a_8 and a_{10} one can use the equations for a_8^c and a_{10}^c given previously to obtain $a_8^{ac} = a_8 - a_8^c$ and $a_{10}^{ac} = a_{10} - a_{10}^c$. Also, the exact values of a_8 and a_8^{ac} for catacondensed benzenoids can be computed by the relationship given by Dias.[35] For molecular graphs of eight vertices or less, it is easy to obtain the matching polynomial by inspection from these coefficient relationships; enumeration of Sachs graphs without cyclic components will frequently allow one to solve for the matching polynomial of slightly larger molecular graphs. Because of the general importance of the characteristic and matching polynomials and their use in determining relative chemical and spectroscopic properties of linear and zigzag conjugated polycyclic hydrocarbons, we will present and study recursion equations for the characteristic and matching polynomials of linear and zigzag conjugated polycyclic hydrocarbon series (Figures 1–2.).

Recursion Equations for the Characteristic and Matching Polynomials of Linear and Zigzag Conjugated Polycyclic Hydrocarbon Series

Figures 1 and 2 presents the linear polyacene and zigzag polyphenacene series and their respective recursion equations for their characteristic and matching polynomials. These recursion equations were derived by Hosoya and Ohkami using an operator technique.[36] The matching recursion equation for linear polyacene series (Figure 1)

$$M_n(X) = (X^4 - 5X^2 + 3)M_{n-1}(X) - (X^4 - 3X^2 + 3)M_{n-2}(X) + M_{n-3}(X) \quad (1)$$

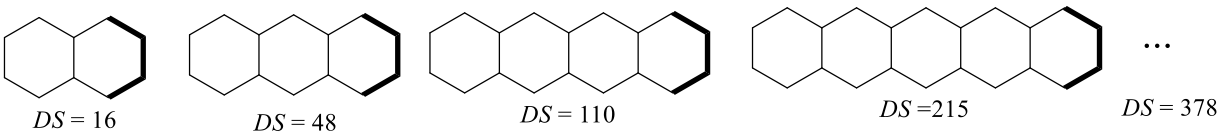

$X^6 - 6X^4 + 9X^2 - 2 = 0$
$X^{10} - 11X^8 + 41X^6 - 61X^4 + 31X^2 - 3 = 0$
$X^{14} - 16X^{12} + 98X^{10} - 290X^8 + 429X^6 - 294X^4 + 76X^2 - 4 = 0$
$X^{18} - 21X^{16} + 180X^{14} - 814X^{12} + 2096X^{10} - 3092X^8 + 2497X^6 - 993X^4 + 155X^2 - 5 = 0$
$M_n(X) = (X^4 - 5X^2 + 3)M_{n-1}(X) - (X^4 - 3X^2 + 3)M_{n-2}(X) + M_{n-3}(X)$

$X^6 - 6X^4 + 9X^2 - 4 = 0$
$X^{10} - 11X^8 + 41X^6 - 65X^4 + 43X^2 - 9 = 0$
$X^{14} - 16X^{12} + 98X^{10} - 296X^8 + 473X^6 - 392X^4 + 148X^2 - 16 = 0$
$X^{18} - 21X^{16} + 180X^{14} - 822X^{12} + 2192X^{10} - 3510X^8 + 3321X^6 - 1731X^4 + 415X^2 - 25 = 0$

$P_n(X) = (X^4 - 5X^2 + 4)[P_{n-1}(X) + P_{n-3}(X)] - (2X^4 - 6X^2 + 6)P_{n-2}(X) - P_{n-4}(X)$

Figure 1. The recursion equations for the linear polyacene series along with the initial requisite number of matching and characteristic polynomials. The auf bau unit is shown in bold.

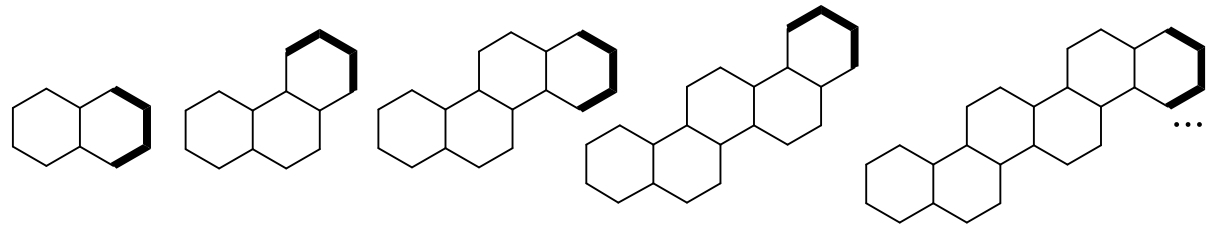

$X^6 - 6X^4 + 9X^2 - 2 = 0$
$X^{10} - 11X^8 + 41X^6 - 61X^4 + 31X^2 - 3 = 0$
$X^{14} - 16X^{12} + 98X^{10} - 291X^8 + 435X^6 - 305X^4 + 82X^2 - 5 = 0$
$X^{18} - 21X^{16} + 180X^{14} - 816X^{12} + 2117X^{10} - 3173X^8 + 2638X^6 - 1102X^4 + 189X^2 - 8 = 0$

$$M_n(X) = (X^4 - 5X^2 + 3)M_{n-1}(X) - (X^4 - 2X^2 + 2)M_{n-2}(X) - (X^4 - 3X^2 + 1)M_{n-3}(X) + M_{n-4}(X)$$

$X^6 - 6X^4 + 9X^2 - 4 = 0$
$X^{10} - 11X^8 + 41X^6 - 65X^4 + 43X^2 - 9 = 0$
$X^{14} - 16X^{12} + 98X^{10} - 297X^8 + 479X^6 - 407X^4 + 166X^2 - 25 = 0$
$X^{18} - 21X^{16} + 180X^{14} - 824X^{12} + 2213X^{10} - 3599X^8 + 3518X^6 - 1972X^4 + 568X^2 - 64 = 0$

$$P_n(X) = (X^4 - 5X^2 + 4)[P_{n-1}(X) + P_{n-4}(X)] - (2X^4 - 5X^2 + 3)[P_{n-2}(X) + P_{n-3}(X)] - P_{n-5}(X)$$

Figure 2. The recursion equations for the zigzag polyphenacene series along with the initial requisite number of matching and characteristic polynomials. The auf bau unit is shown in bold.

requires one to know the matching polynomials for the three prior linear members of the series [M_{n-1}(X), M_{n-2}(X), and M_{n-3}(X)] to obtain the next member [M_n(X)]. The characteristic recursion equation for linear polyacene series (Figure 1)

$$P_n(X) = (X^4 - 5X^2 + 4)[P_{n-1}(X) + P_{n-3}(X)] - (2X^4 - 6X^2 + 6)P_{n-2}(X) - P_{n-4}(X) \quad (2)$$

requires one to know the characteristic polynomials for the four prior members of the series

[P_{n-1}(X), P_{n-2}(X), P_{n-3}(X), and P_{n-4}(X)] to obtain the next member [P_n(X)]. Benzene is the first member, and its respective polynomials can be used to start these recursion equations.

The matching recursion equation for polyphenacene series (Figure 2)

$$M_n(X) = (X^4 - 5X^2 + 3)M_{n-1}(X) - (X^4 - 2X^2 + 2)M_{n-2}(X) - (X^4 - 3X^2 + 1)M_{n-3}(X) + M_{n-4}(X) \quad (3)$$

requires one to know the matching polynomials for the four prior member of the series [M_{n-1}(X), M_{n-2}(X), M_{n-3}(X),and M_{n-4}(X)] to obtain the next member [M_n(X)]. The characteristic recursion equation for zigzag polyphenacene series (Figure 2)

$$P_n(X) = (X^4 - 5X^2 + 4)[P_{n-1}(X) + P_{n-4}(X)] - (2X^4 - 5X^2 + 3)[P_{n-2}(X) + P_{n-3}(X)] - P_{n-5}(X) \quad (4)$$

requires one to know the characteristic polynomials for the five prior zigzag members of the series [P_{n-1}(X), P_{n-2}(X), P_{n-3}(X), P_{n-4}(X), and P_{n-5}(X)] to obtain the next member [P_n(X)]. Benzene is the first member, and its respective polynomials can be used to start these recursion equations. Overall, the phenacene recursion equations require one more member term to compute the characteristic and matching polynomials for the phenacene series. We will show that these recursion equations can be applied directly or with some modification to other related series.

Recursion Equations for the Characteristic and Matching Polynomials of Conjugated Systems Related to Linear Conjugated Polycyclic Hydrocarbon Series

The linear polyacene related systems given in Figure 3 have been studied previously in other regards. All four of the linear series in Figure 3 have been studied by Aihara and coworkers.[27,29] E_π is obtained from the characteristic polynomial and E_π(ref) is obtained from the matching polynomial. The characteristic and matching polynomials for members of the upper two series having up to seven rings can be found in the work of Hosoya and coworkers.[37,38] The polyacene-2,3-quinododimethide series

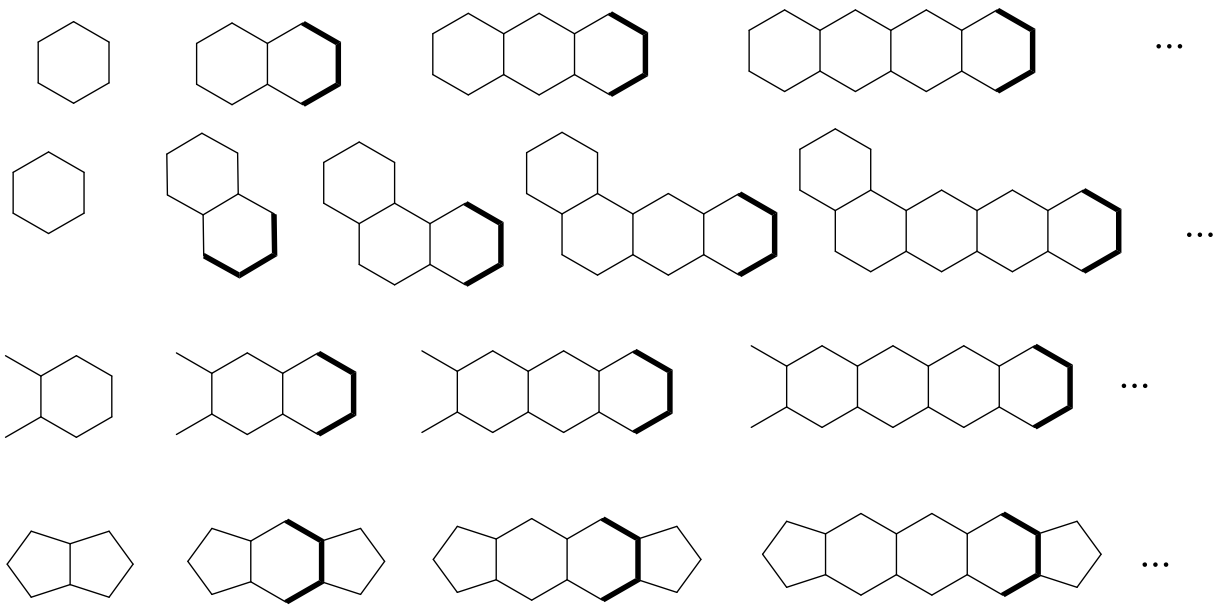

$$M_n(\mathrm{X}) = (\mathrm{X}^4 - 5\mathrm{X}^2 + 3)M_{n-1}(\mathrm{X}) - (\mathrm{X}^4 - 3\mathrm{X}^2 + 3)M_{n-2}(\mathrm{X}) + M_{n-3}(\mathrm{X})$$

$$P_n(\mathrm{X}) = (\mathrm{X}^4 - 5\mathrm{X}^2 + 4)[P_{n-1}(\mathrm{X}) + P_{n-3}(\mathrm{X})] - (2\mathrm{X}^4 - 6\mathrm{X}^2 + 6)P_{n-2}(\mathrm{X}) - P_{n-4}(\mathrm{X})$$

Figure 3. The recursion equations for the linear related polyacene series along with the initial requisite number of members whose matching and characteristic polynomials that need to be known. All these series obey the same recursion equations. The auf bau unit is shown in bold. In the last series, the auf bau unit involves insertion.

(third series in Figure 3) has been studied in terms of aromaticity and diatropicity[27] and conjugation and Dewar resonance structures.[28] This series has further importance in that the eigenvalues of its members correspond to the doubly degenerate HMO eigenvalues of the [*n*]cyclacenes where *n* is an odd number of rings. For *n* = even number of rings Figure 4 illustrates two different right-hand fragments that are strongly subspectral. The upper part of Figure 4 displays two perpendicular mirror-plane fragmentation of [10]cyclacene which gives the right-hand mirror-plane fragments corresponding the third member of this series. In this example, the mirror plane is perpendicular to the plane of the paper and bisects through a valley to a valley on the left and through a peak to a peak on the right. The lower part of Figure 4 gives the corresponding mirror-plane fragments for [10]cyclacenes. In this case, perpendicular mirror-plane fragmentation leads to right-hand fragments that are strongly subspectral mates whose eigenvalues correspond to one set of the doubly degenerate eigenvalues.[39] For the perpendicular mirror-plane which goes from peak to peak, one will get tetracene which has the same eigenvalues, except instead of the doubly degenerate zero eigenvalues it has the eigenvalues of ± 1.[40] What this mirror-plane fragmentation shows are that cyclacenes with an even number of rings are HMO diradicals but can be drawn with four different classical structures or Kekulé structures (i.e., ***K*** = 4). We have previously argued that whenever a polycyclic conjugated molecule can be drawn with all its π–electrons paired but are computed to be HMO diradicals that the actual molecule must be an open-shell singlet.[41] This is in complete agreement with higher level calculations (UBS-B3LYP).[42] Figure 5 gives the matching and characteristic polynomials for the polyacene-2,3-quinododimethides. Members of this series were calculated by the B3LYP method to have substantial diradical character with pentacene-2,3-quinododimethide having the most diradical character which thereafter progressively decreased as the number of rings increased.[43] While the members of this series derive from mirror-plane fragmentation of cyclacenes with an odd number of rings, their bandgap more rapidly approaches zero than do the linear polyacenes, e.g., HOMO = –LUMO = 0.075338 β for tetracene-2,3-quinododimethides (fourth structure in Figure 5) compared to HOMO = –LUMO = 0.2950 β for tetracene (third structure in Figure 1). Since the largest linear polyacene, nonacene, is predicted to have an open-shell singlet diradical ground state, the comparable sized cyclacenes are expected to also be open-shell singlets. The preparation and characterization of nonacene to undecacene have been reported.[44,45] However, the preparative scale synthesis of larger linear polyacene homologues remain a formidable challenge.

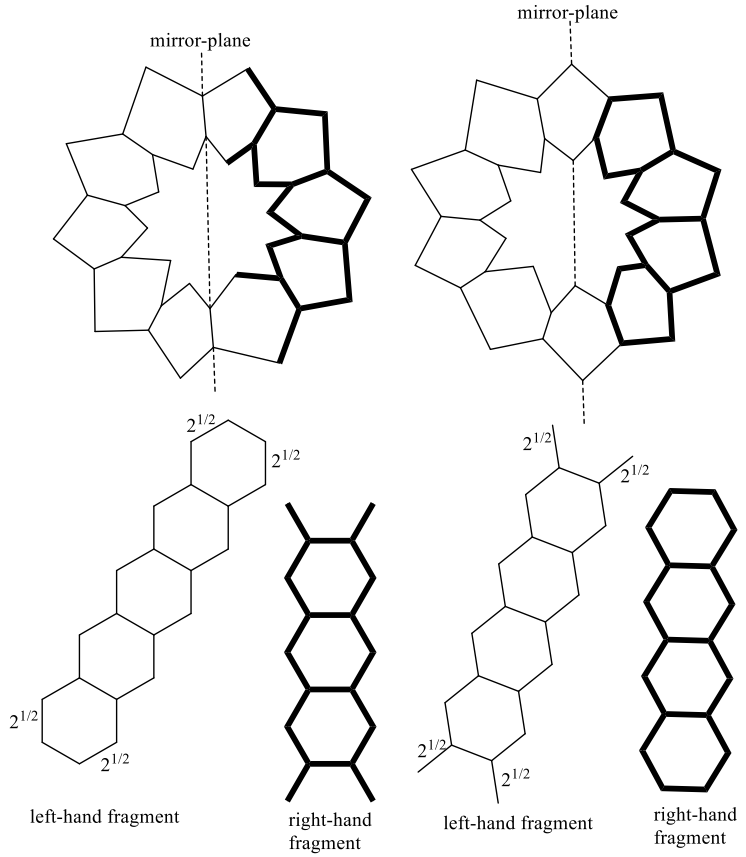

Figure 4. Schlegel of [10]cyclacene ($C_{40}H_{20}$) and its valley-to-valley and peak-to-peak fragmentations. The right-hand fragment is shown in bold and is the origin of the antisymmetric eigenvalues and corresponding eigenvectors. The left-hand fragment is the origin of the symmetric eigenvalues and corresponding eigenvectors. The 2,3,6,7-tetramethylenylanthracene and tetracene are embedding fragments.

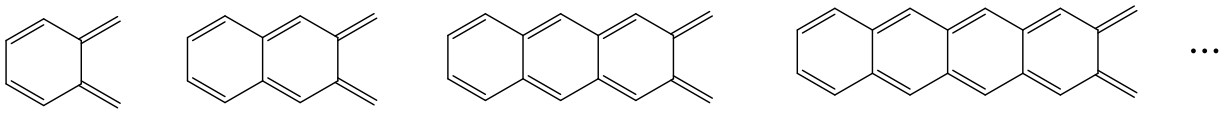

$$X^8 - 8X^6 + 18X^4 - 11X^2 + 1 = 0$$
$$X^{12} - 13X^{10} + 60X^8 - 119X^6 + 97X^4 - 26X^2 + 1 = 0$$
$$X^{16} - 18X^{14} + 127X^{12} - 447X^{10} + 827X^8 - 779X^6 + 335X^4 - 50X^2 + 1 = 0$$
$$X^{20} - 23X^{18} + 219X^{16} - 1120X^{14} + 3341X^{12} - 5917X^{10} + 6078X^8 - 3396X^6 + 904X^4 - 85X^2 + 1 = 0$$
$$M_n(X) = (X^4 - 5X^2 + 3)M_{n-1}(X) - (X^4 - 3X^2 + 3)M_{n-2}(X) + M_{n-3}(X)$$

$$X^8 - 8X^6 + 18X^4 - 13X^2 + 1 = 0$$
$$X^{12} - 13X^{10} + 60X^8 - 123X^6 + 113X^4 - 38X^2 + 1 = 0$$
$$X^{16} - 18X^{14} + 127X^{12} - 453X^{10} + 879X^8 - 921X^6 + 475X^4 - 90X^2 + 1 = 0$$
$$X^{20} - 23X^{18} + 219X^{16} - 1128X^{14} + 3449X^{12} - 6457X^{10} + 7334X^8 - 4792X^6 + 1580X^4 - 185X^2 + 1 = 0$$
$$P_n(X) = (X^4 - 5X^2 + 4)[P_{n-1}(X) + P_{n-3}(X)] - (2X^4 - 6X^2 + 6)P_{n-2}(X) - P_{n-4}(X)$$

Figure 5. Matching and characteristic polynomials for the polyacene-2,3-quinododimethide series for the initial requisite number of members that need to be known for application of the listed recursion equations. Compare with the right-hand fragment of [9]cyclacene.

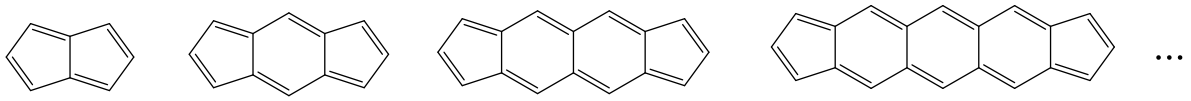

$$X^8 - 9X^6 + 24X^4 - 20X^2 + 2 = 0$$
$$X^{12} - 14X^{10} + 71X^8 - 160X^6 + 157X^4 - 52X^2 + 2 = 0$$
$$X^{16} - 19X^{14} + 143X^{12} - 545X^{10} + 1116X^8 - 1198X^6 + 600X^4 - 104X^2 + 2 = 0$$
$$X^{20} - 24X^{18} + 240X^{16} - 1300X^{14} + 4154X^{12} - 7998X^{10} + 9089X^8 - 5704X^6 + 1717X^4 - 180X^2 + 2 = 0$$
$$M_n(X) = (X^4 - 5X^2 + 3)M_{n-1}(X) - (X^4 - 3X^2 + 3)M_{n-2}(X) + M_{n-3}(X)$$

$$X^8 - 9X^6 + 24X^4 - 4X^3 - 20X^2 + 8X = 0$$
$$X^{12} - 14X^{10} + 71X^8 - 4X^7 - 162X^6 + 28X^5 + 165X^4 - 52X^3 - 56X^2 + 24X = 0$$
$$X^{16} - 19X^{14} + 143X^{12} - 4X^{11} - 549X^{10} + 48X^9 + 1152X^8 - 200X^7 - 1300X^6 + 356X^5 + 700X^4 - 256X^3 - 120X^2 + 48X = 0$$
$$X^{20} - 24X^{18} + 240X^{16} - 4X^{15} - 1306X^{14} + 68X^{13} + 4238X^{12} - 448X^{11} - 8436X^{10} + 1468X^9 + 10153X^8 - 2544X^7 - 6922X^6 + 2252X^5 + 2269X^4 - 864X^3 - 220X^2 + 80X = 0$$
$$P_n(X) = (X^4 - 5X^2 + 4)[P_{n-1}(X) + P_{n-3}(X)] - (2X^4 - 6X^2 + 6)P_{n-2}(X) - P_{n-4}(X)$$

Figure 6. Matching and characteristic polynomials for the dicyclopenta-fused polyacene series for the initial requisite number of members that need to be known for application of the listed recursion equations. Compare with recursion equations in Figure 3.

The dicyclopenta-fused polyacene series in Figure 6 begins with pentalene which is antiaromatic and has only been synthesized in argon matrices and studied.[46] Since pentalene can be written with two classical structures but is a HMO diradical, it is predicted to be an open-shell singlet. All members of this series have a 4*n* pπ-electron perimeter with two Kekulé resonance structures (***K*** = 2) and larger members of this series have been predicted by various methods as becoming increasingly aromatic because of recovery of aromaticity of the middle section. For larger members of this Figure 6 series, it was argued that allyl-polyacene-allyl biradical structures prevailed, owing to larger resonance energies.[47] It was shown that intercalating benzene rings in going from pentalene to dicyclopenta[*b,g*]naphthalene, there was a change from the localized structure of pentalene to a delocalized structure.of dicyclopenta[*b,g*]naphthalene.[48] The dicyclo-penta-fused polyacenes (Figure 6) linear series have been studied by Makino and Aihara in regard to their aromaticity and magnetotropicity.[29] They showed that the insertion of an increasing number of hexagonal rings into the pentalene moiety led to higher members of increasing aromaticity and diatropicity due to the collective effect of non-conjugated *circuits*.

While all the linear related series in Figure 3 obey precisely the same recursion equations, the linear series in Figures 7 and 8 obey a slightly modified version of these recursions with the indicated additional end constant terms. The polyacene-2,x-quinododimetide series (Figure 7) has been studied in regard their progressive aromaticity and diatropicity change with increasing size and in regard to their conjugation as a function of their number of Dewar resonance structures.[28,29] Both these series possess no Hamiltonian circuit or path whereas those in Figure 3 do.

Recursion Equations for the Characteristic and Matching Polynomials of Conjugated Systems Related to Zigzag Phenacene Conjugated Polycyclic Hydrocarbon Series

The zigzag phenacene related series in Figure 9 all obey the same recursion equations for characteristic polynomial; the first three series also obey the same matching recursion equation. The first phenacene series (uppermost series in Figure 9) has been extensively studied by Hosoya and coworkers.[36] The polyphenacene-1,x-quinododimethide series (second series) have been studied in regard to conjugation and were shown to be right-hand mirror-plane fragments belonging to a series of fullerenes having rotational symmetry that were generated by circumscribing.[49] Figure 10 summarizes the matching and characteristic polynomials of the first several members and respective recursion equations.

The last weighted vertex polyphenacene related series (Figure 9) are also right-hand mirror-plane fragments belonging to a series of carbon clusters and fullerenes having rotational symmetry that were generated by circumscribing.[50] Here the vertex weights are minus one (–1). The third row in Figure 9 are mirror-plane fragments to the monocapped nanotubes in Figure 11. Figure 12

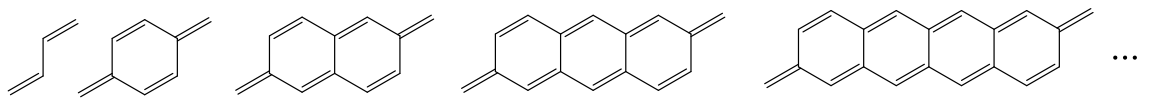

$X^4 - 3X^2 + 1 = 0$
$X^8 - 8X^6 + 18X^4 - 10X^2 + 1 = 0$
$X^{12} - 13X^{10} + 60X^8 - 118X^6 + 92X^4 - 22X^2 + 1 = 0$
$X^{16} - 18X^{14} + 127X^{12} - 446X^{10} + 817X^8 - 748X^6 + 303X^4 - 40X^2 + 1 = 0$
$X^{20} - 23X^{18} + 219X^{16} - 1119X^{14} + 3326X^{12} - 5834X^{10} + 5869X^8 - 3155X^6 + 785X^4 - 65X^2 + 1 = 0$
$X^{24} - 28X^{22} + 336X^{20} - 2262X^{18} + 9394X^{16} - 24940X^{14} + 42482X^{12} - 45478X^{10} + 29229X^8 - 10380X^6 + 1743X^4 - 98X^2 + 1 = 0$
$M_n(X) = (X^4 - 5X^2 + 3)M_{n-1}(X) - (X^4 - 3X^2 + 3)M_{n-2}(X) + M_{n-3}(X) + X^2$

$X^8 - 8X^6 + 18X^4 - 12X^2 + 1 = 0$
$X^{12} - 13X^{10} + 60X^8 - 122X^6 + 108X^4 - 32X^2 + 1 = 0$
$X^{16} - 18X^{14} + 127X^{12} - 452X^{10} + 869X^8 - 888X^6 + 431X^4 - 70X^2 + 1 = 0$
$X^{20} - 23X^{18} + 219X^{16} - 1127X^{14} + 3434X^{12} - 6372X^{10} + 7101X^8 - 4467X^6 + 1365X^4 - 135X^2 + 1 = 0$
$X^{24} - 28X^{22} + 336X^{20} - 2272X^{18} + 9578X^{16} - \sigma\ 26294X^{14} + 47614X^{12} - 56232X^{10} + 41657X^8 - 17826X^6 + 3703^4 - 238X^2 + 1 = 0$
$P_n(X) = (X^4 - 5X^2 + 4)[P_{n-1}(X) + P_{n-3}(X)] - (2X^4 - 6X^2 + 6)P_{n-2}(X) - P_{n-4}(X) + 2X^2$

Figure 7. Polyacene-2,x-quinododimethide series. Note the end terms need to be determined by inspection to bring in agreement the recursions equations. These ring structures have no Hamiltonian path.

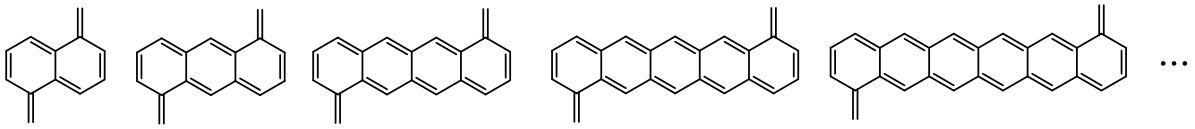

$X^8 - 8X^6 + 18X^4 - 10X^2 + 1 = 0$
$X^{12} - 13X^{10} + 60X^8 - 120X^6 + 100X^4 - 27X^2 + 1 = 0$
$X^{16} - 18X^{14} + 127X^{12} - 448X^{10} + 835X^8 - 798X^6 + 350X^4 - 52X^2 + 1 = 0$
$X^{20} - 23X^{18} + 219X^{16} - 1121X^{14} + 3354X^{12} - 5978X^{10} + 6206X^8 - 3516X^6 + 945X^4 - 86X^2 + 1 = 0$
$X^{24} - 28X^{22} + 336X^{20} - 2264X^{18} + 9432X^{16} - 25228X^{14} + 43599X^{12} - 47846X^{10} + 31954X^8 - 11982X^6 + 2157X^4 - 130X^2 + 1 = 0$
$X^{28} - 33X^{26} + 478X^{24} - 4002X^{22} + 21469X^{20} - 77333X^{18} + 190662X^{16} - 322140X^{14} + 367906X^{12} - 275670X^{10} + 128653X^8 - 34189X^6 + 4376X^4 - 185X^2 + 1 = 0$
$M_n(X) = (X^4 - 5X^2 + 3)M_{n-1}(X) - (X^4 - 3X^2 + 3)M_{n-2}(X) + M_{n-3}(X) + (X^6 - 2X^4 + X^2)$

$X^8 - 8X^6 + 18X^4 - 12X^2 + 1 = 0$
$X^{12} - 13X^{10} + 60X^8 - 124X^6 + 116X^4 - 41X^2 + 1 = 0$
$X^{16} - 18X^{14} + 127X^{12} - 454X^{10} + 887X^8 - 942X^6 + 498X^4 - 100X^2 + 1 = 0$
$X^{20} - 23X^{18} + 219X^{16} - 1129X^{14} + 3462X^{12} - 6520X^{10} + 7482X^8 - 4968X^6 + 1677X^4 - 202X^2 + 1 = 0$
$X^{24} - 28X^{22} + 336X^{20} - 2274X^{18} + 9616X^{16} - 26586X^{14} + 48799X^{12} - 59004X^{10} + 45450X^8 - 20726X^6 + 4777X^4 - 362X^2 + 1 = 0$
$X^{28} - 33X^{26} + 478X^{24} - 4014X^{22} + 21749X^{20} - 80075X^{18} + 205402X^{16} - 369918X^{14} + 464474X^{12} - 397224X^{10} + 220849X^8 - 73109X^6 + 12016X^4 - 597X^2 + 1 = 0$
$P_n(X) = (X^4 - 5X^2 + 4)[P_{n-1}(X) + P_{n-3}(X)] - (2X^4 - 6X^2 + 6)P_{n-2}(X) - P_{n-4}(X) + 2(X^6 - 2X^4 + X^2)$

Figure 8. Polyacene-1,x-quinododimethide series. Note the end terms need to be determined by inspection to bring in agreement the recursions equations. Except for the first member, these structures are devoid of Hamiltonian paths.

presents the matching and characteristic polynomials of the first several mirror-plane members and respective recursion equations. These odd carbon clusters are precursors to fullerene series generated by successive circumscribing where the higher members become elongated with increasing size to form bicapped nanotubes.

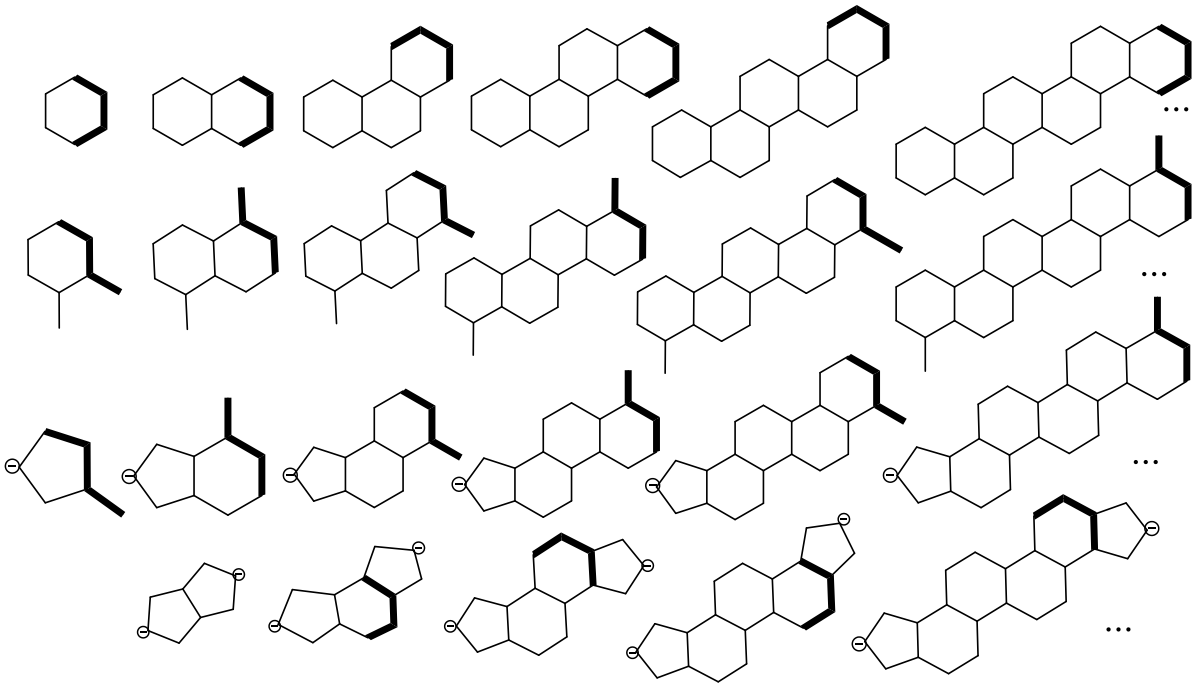

$$P_n(X) = (X^4 - 5X^2 + 4)[P_{n-1}(X) + P_{n-4}(X)] - (2X^4 - 5X^2 + 3)[P_{n-2}(X) + P_{n-3}(X)] - P_{n-5}(X)$$

$$M_n(X) = (X^4 - 5X^2 + 3)M_{n-1}(X) - (X^4 - 2X^2 + 2)M_{n-2}(X) - (X^4 - 3X^2 + 1)M_{n-3}(X) + M_{n-4}(X)$$

Figure 9. The recursion equations for the zigzag related polyphenacene series. The initial requisite number of members whose polynomials need to be known for the upper three series are given in Figures 2, 10, and 12. The first three series obey the same the same recursion equations for the characteristic and matching polynomials. The fourth series obeys the same recursion equation for the characteristic polynomial but its compliance with the matching polynomial is unknown.

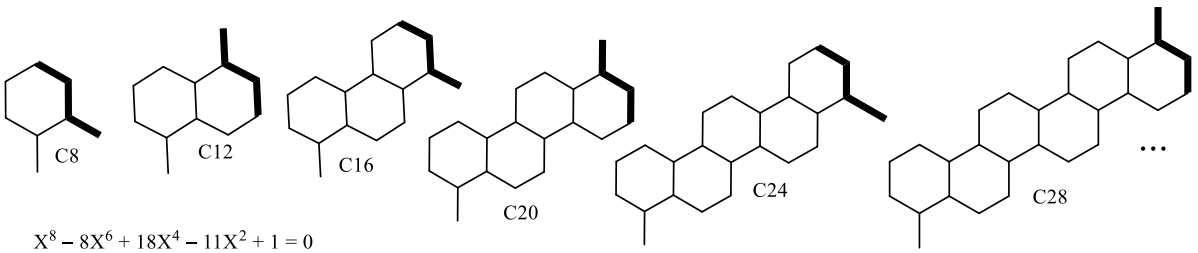

$$X^8 - 8X^6 + 18X^4 - 11X^2 + 1 = 0$$

$$X^{12} - 13X^{10} + 60X^8 - 120X^6 + 100X^4 - 27X^2 + 1 = 0$$

$$X^{16} - 18X^{14} + 127X^{12} - 449X^{10} + 843X^8 - 818X^6 + 366X^4 - 56X^2 + 1 = 0$$

$$X^{20} - 23X^{18} + 219X^{16} - 1123X^{14} + 3380X^{12} - 6103X^{10} + 6482X^8 - 3800X^6 + 1073X^4 - 106X^2 + 1 = 0$$

$$M_n(X) = (X^4 - 5X^2 + 3)M_{n-1}(X) - (X^4 - 2X^2 + 2)M_{n-2}(X) - (X^4 - 3X^2 + 1)M_{n-3}(X) + M_{n-4}(X)$$

$$X^8 - 8X^6 + 18X^4 - 13X^2 + 1 = 0$$

$$X^{12} - 13X^{10} + 60X^8 - 124X^6 + 116X^4 - 41X^2 + 1 = 0$$

$$X^{16} - 18X^{14} + 127X^{12} - 455X^{10} + 895X^8 - 966X^6 + 530X^4 - 116X^2 + 1 = 0$$

$$X^{20} - 23X^{18} + 219X^{16} - 1131X^{14} + 3488X^{12} - 6653X^{10} + 7830X^8 - 5464X^6 + 2045X^4 - 314X^2 + 1 = 0$$

$$P_n(X) = (X^4 - 5X^2 + 4)[P_{n-1}(X) + P_{n-4}(X)] - (2X^4 - 5X^2 + 3)[P_{n-2}(X) + P_{n-3}(X)] - P_{n-5}(X)$$

Figure 10. Matching and characteristic polynomials for the polyphenacene-1,x-quinododimethide series for the initial requisite number of members that need to be known for application of the listed recursion equations. Compare with Figure 9.

The last row of Figure 9 are mirror-plane fragments bicapped fullerene nanotubes. The recursion equation for the characteristic polynomial of the last series has been published.[50] Figure 13 summarize the eigenvalues for these fragments of the bicapped fullerene nanotubes also listed in Figure 9. The last three series give the doubly

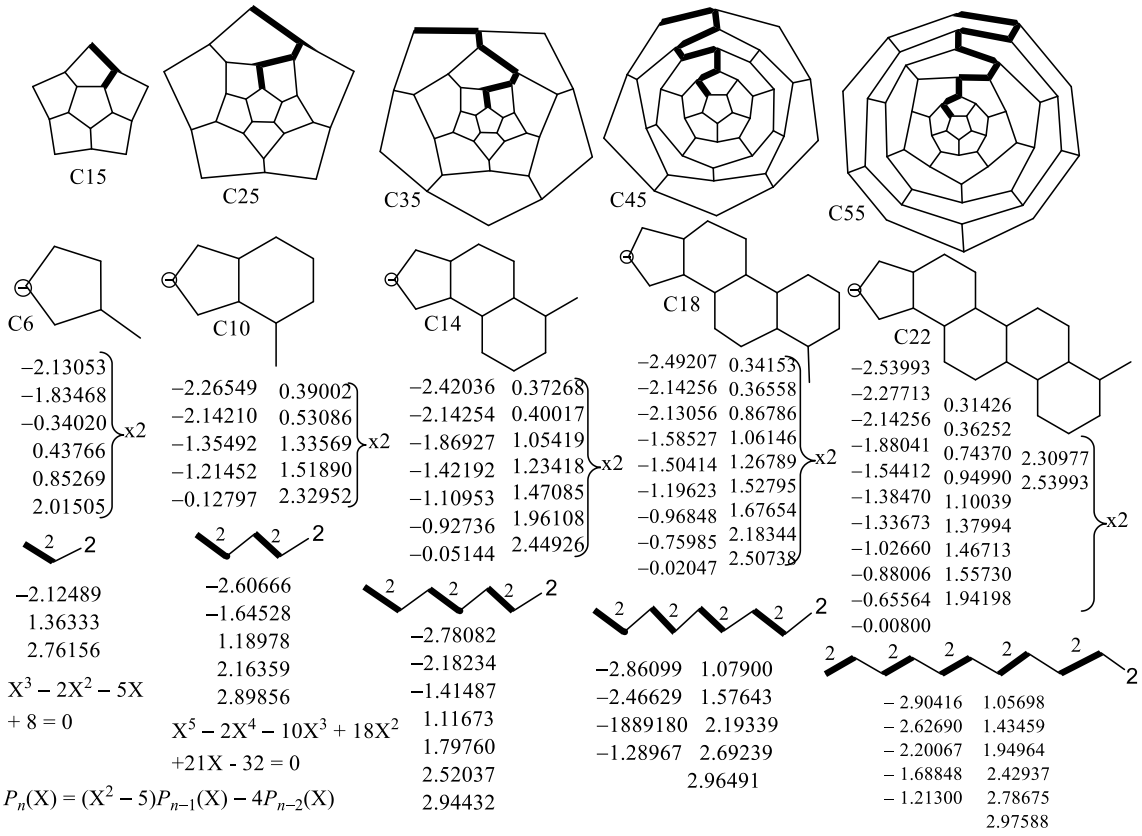

Figure 11. The above monocapped carbon cluster can serve as precursors to bicapped nanotubes through their dimerization.

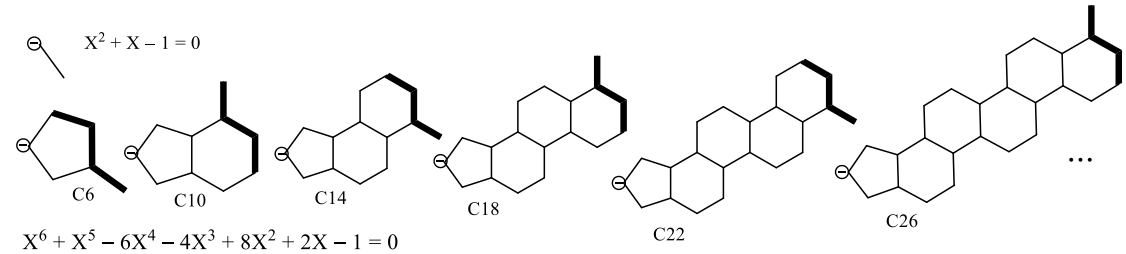

$X^6 + X^5 - 6X^4 - 4X^3 + 8X^2 + 2X - 1 = 0$

$X^{10} + X^9 - 11X^8 - 9X^7 + 40X^6 + 24X^5 - 56X^4 - 20X^3 + 25X^2 + 4X - 1 = 0$

$X^{14} + X^{13} - 16X^{12} - 14X^{11} + 97X^{10} + 71X^9 - 281X^8 - 161X^7 + 402X^6 + 163X^5 - 261X^4 - 65X^3 + 58X^2 + 7X - 1 = 0$

$X^{18} + X^{17} - 21X^{16} - 19X^{15} + 179X^{14} + 143X^{13} - 801X^{12} - 547X^{11} + 2033X^{10} + 1136X^9 - 2947X^8 - 1270X^7 + 2325X^6 + 714X^5 - 880X^4 - 172X^3 + 117X^2 + 12X - 1 = 0$

$M_n(X) = (X^4 - 5X^2 + 3)M_{n-1}(X) - (X^4 - 2X^2 + 2)M_{n-2}(X) - (X^4 - 3X^2 + 1)M_{n-3}(X) + M_{n-4}(X)$

$X^6 + X^5 - 6X^4 - 4X^3 + 8X^2 - 1 = 0$

$X^{10} + X^9 - 11X^8 - 9X^7 + 40X^6 + 22X^5 - 58X^4 - 14X^3 + 29X^2 - 4X - 1 = 0$

$X^{14} + X^{13} - 16X^{12} - 14X^{11} + 97X^{10} + 69X^9 - 285X^8 - 147X^7 + 428X^6 + 129X^5 - 311X^4 - 23X^3 + 86X^2 - 15X - 1 = 0$

$X^{18} + X^{17} - 21X^{16} - 19X^{15} + 179X^{14} + 141X^{13} - 807X^{12} - 525X^{11} + 2101X^{10} + 1046X^9 - 3225X^8 - 1078X^7 + 2837X^6 + 466X^5 - 1300X^4 + 12X^3 + 237X^2 - 44X - 1 = 0$

$X^{22} + X^{21} - 26X^{20} - 24X^{19} + 286X^{18} + 238X^{17} - 1749X^{16} - 1273X^{15} + 6573X^{14} + 4022X^{13} - 15828X^{12} - 7704X^{11} + 24657X^{10} + 8749X^9 - 24430X^8 - 5342X^7 + 14648X^6 + 1184X^5 - 4765X^4 + 268X^3 + 634X^2 - 120X - 1 = 0$

$P_n(X) = (X^4 - 5X^2 + 4)P_{n-1}(X) - (2X^4 - 5X^2 + 3)[P_{n-2}(X) + P_{n-3}(X)] + (X^4 - 5X^2 + 4)P_{n-4}(X) - P_{n-5}(X)$

Figure 12. Matching and characteristic polynomials for the mirror-plane fragments to monocapped carbon clusters in Figure 11. Also, compare with Figure 9.

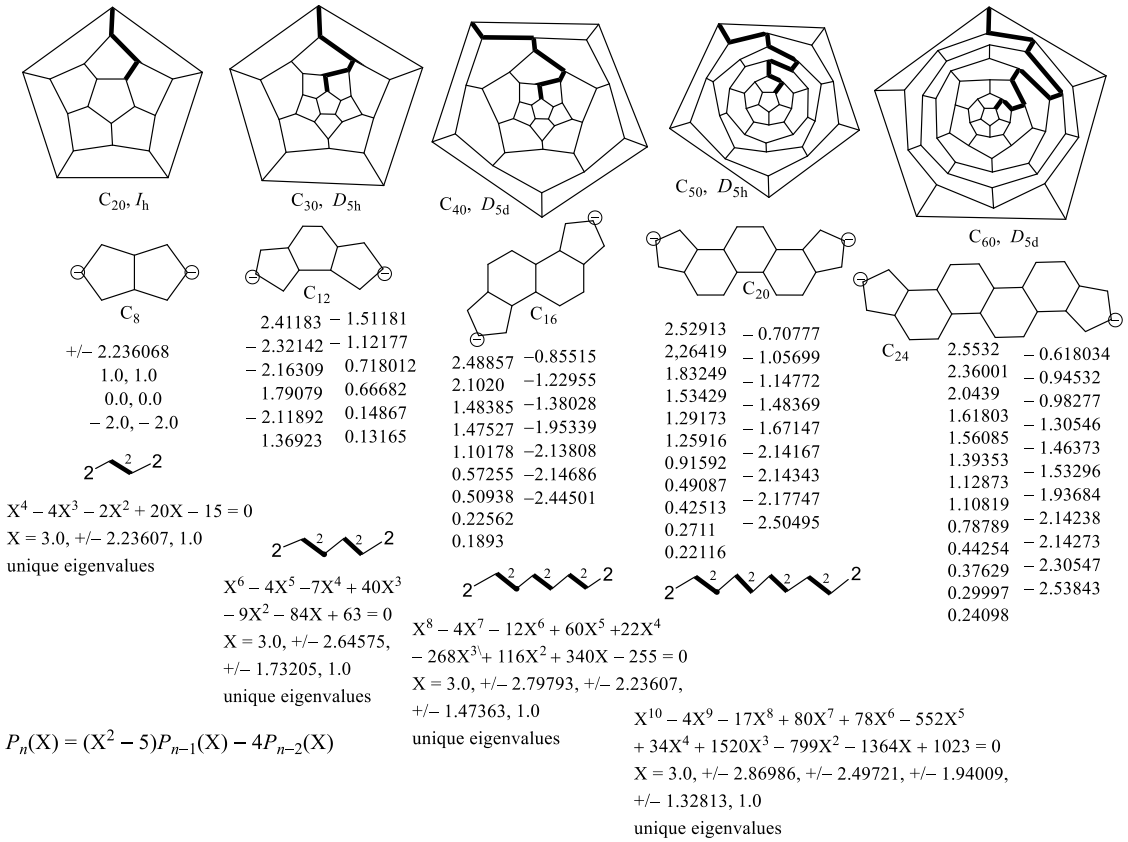

Figure 13. Fullerene series that become elongated fullerene tubes with increasing size.

degenerate eigenvalues to the corresponding nanotube, monocapped, and bicapped fullerene nanotubes.[49,50] Sufficient amounts of [10]phenacene and [11]phenacene have been synthesized using a simple repetition of Wittig reactions followed by photocyclization.[51]

An alternative method of constructing bicapped nanotubes is by joining any two monocapped carbon clusters at their open ends in Figure 11. Dimerizing two C15 carbon clusters gives the C30 nanotube in Figure 13. Joining the C15 carbon cluster with the C25 carbon cluster gives the C40 nanotube in Figure 13. Dimerizing two C25 carbon clusters gives the C50 nanotube, and proceeding so forth will give the whole Figure 13 nanotube series.

Conjugation Versus Aromaticity and Equations for Number of Dewar Resonance Structures (*DS*s) in Polycyclic Aromatic Series

Table 1 list the TRE and TCE values for the Figures 5 and 6 series and the edge deleted successor series for the poly-*s*-indacene series of Figure 6 in Figure 14. Pentalene can be regarded as the first member of this series, *s*-indacene as the second, and dicyclopenta[*b*,*g*]naphthalene as the third. Deletion of one bond in pentalene gives 1-vinylfulvene and two bonds gives [4]dendralene all with the same number of pπ-bonds which are the lead members in Figures 14 and 15. The succession of values for TRE is –0. 215, 0.0144, and 0 β and for TCE is 2.671, 1.925, and 1.332 β, respectively. The reason that 2-vinylfulvene is slightly aromatic rather than nonaromatic is due to the anionic polar cyclopentadiene circuit contribution that occurs in this nonalternant hydrocarbons. Pentalene is significantly antiaromatic and [4]dendralene is the least conjugated pπ systems. For comparison, the TRE = BRE = –0.595 β and TCE = 2.252 β for antiaromatic cyclocta-1,3,5,7-tetraene. Formation of pentalene by bridging two nonstarred positions in cyclocta-1,3,5,7-tetraene results in less antiaromaticity (TRE goes from to –0.595 to –0. 215 β) and more conjugation (TCE goes from 2.252 to 2.671 β). All the TCE values in Table 1 are larger than the corresponding TRE values. These numerical results are consistent with our chemical anticipation.

s-Indacene and higher homologs (Figure 6) become increasingly more aromatic due to increasing number of benzene rings (r_6) and Dewar resonances structures [$DS = 1/3(2r_6^3 + 24r_6^2 + 58r_6 + 36)$]. This alternative explanation for the increasing aromaticity of the Figure 6 dicyclopenta-polyacene series should be compared to allyl-polyacene-

Table 1. Valence-Bond electronic properties of compounds in Figures 5, 6, 14, and 15.

Polyacene-2,3-quinododimethides	TRE, β (%TRE)	TCE, β	TCE/double bond, β	No. double bonds; No. rings	DS
Benzene-	0.059 (0.599)	1.8947	0.4737	4; 1	7
Naphthalene-	0.140 (0.913)	3.3910	0.5652	6; 2	20
Anthracene-	0.225 (1.078)	4.9074	0.6134	8; 3	42
Naphthacene-	0.309 (1.169)	6.4318	0.6432	10; 4	75
Pentacene-	0.391 (1.224)	7.9601	0.6633	12; 5	121
Hexacene-	0.472 (1.258)	9.4904	0.6779	14, 6	182
Dicyclopentapolyacenes					
(Pentalene)	(–0.215) (–2.02)	(2.6708)	(0.6677)	(4; 2)	(12)
Benzene	0.055 (0.34)	4.1767	0.6961	6; 3	40
Naphthalene	0.192 (0.89)	5.6974	0.7122	8; 4	88
Anthracene	0.292 (1.07)	7.2241	0.7224	10; 5	160
Naphthacene	0.379 (1.16)	8.7536	0.7295	12; 6	260
Pentacene	0.461 (1.20)			14, 7	392
Hexacene	0.541 (1.24)			16, 8	560
Cyclopenta-3-vinyl,2-methylenylpolyacenes					
5-methylene-1-vinylcyclopenta-1,3-diene	0.0144 (0.1451)	1.9248	0.4812	4; 1	8
5-methylene-6-vinyl-5*H*-indene	0.0849 (0.5502)	3.4310	0.5683	6; 2	23
6-methylene-7-vinyl-6*H*-cyclopenta[*b*]naphthalene	0.1646 (0.7856)	4.9512	0.6189	8; 3	48
7-methylene-8-vinyl-7*H*-cyclopenta[*b*]anthracene	0.2484 (0.9381)	6.4783	0.6478	10; 4	85
3,y-Divinyl-polyacene-2,x-quinododimethides					
Benzene (x = 5, y = 6)	0.0442 (0.2989)	2.7878	0.4646	6; 1	10
Naphthalene (x = 6, y = 7)	0.1094 (0.5394)	4.2816	0.5352	8; 2	22
Anthracene (x = 7, y = 8)	0.1834 (0.7111)	5.7915	0.5792	10; 3	40
Naphthacene (x = 8, y = 9)	0.2606 (0.8323)	7.3098	0.6092	12; 4	65

allyl biradical structures explanation of Havenith *et al.*, and Makino and Aihara collective contribution of non-conjugated circuits explanation.[29,47] Per Table 1 the TCE /double bond is increasing with increasing length of the dicyclopentapolyacene due to increasing number of benzene rings (r_6) and Dewar resonance structures as determined by the above formula.

Figures 16 and 17 give two different derivations for determining for number of Dewar resonance structures in the linear polyacene series. Figure 16 demonstrates the general derivation of the analytical expressions using successive subtraction. This subtraction starts with known *DS* values of initial members of the linear polyacene series. Successive subtraction is performed until the differences become constant. In the case for the linear polyacene series, the fourth subtraction iteration gives constant differences of 2. The highest power term in the analytical expression equals the number of subtraction iterations. The coefficient of the highest power term equals the constant difference value which also coincides with the Kekulé value (***K***) of the smallest cyclic member of the series; ***K*** = 2 for benzene. The denominator in the analytical expression is the factorial of the highest power value. The remaining coefficients are determined by matrix algebra.

Figure 17 shows the derivation of the recursion expression for the linear polyacene series. We start with recursion equation for the general matching polynomial for the linear polyacene series derived by Hosoya and Ohkami Operator Technique.[36] The tail coefficients of the matching polynomial per the equation $DS = |a_{N-2}^{ac}| - (N/2)\boldsymbol{K}$ gives the Dewar resonance structures (*DS*).[21,28] Thus, the recursion equation for the number of Dewar resonance structures (*DS*) takes the same form as the general matching polynomial recursion equation where the end term must be solved by inspection. In this case, solving several initial members where the end term is an unknown variable and observing the pattern this variable gives the result of $2r + 3$. Comparing the results of the Figure 17 recursion and the Figure 16 analytical expression gives total agreement.

Using the method of successive differences to derive an analytical expression for the phenacene series (zigzag polyacene series) was not successful. However, starting with the recursion equation for the general matching polynomial for the phenacene series as shown in Figure 18 was successful in generating the recursion equation for the number of Dewar resonance structures (*DS*). The recursion equation for *DS* has the same form as the recursion equation for the general matching polynomial where the tail term is determined separately. The numerical values of

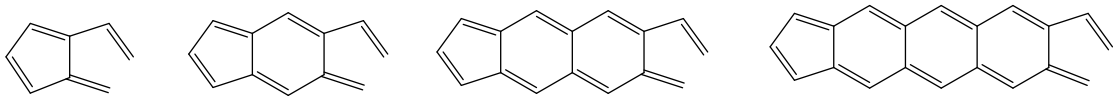

$X^8 - 8X^6 + 18X^4 - 12X^2 + 1 = 0$

$X^{12} - 13X^{10} + 60X^8 - 120X^6 + 102X^4 - 29X^2 + 1 = 0$

$X^{16} - 18X^{14} + 127X^{12} - 448X^{10} + 837X^8 - 809X^6 + 362X^4 - 56X^2 + 1 = 0$

$X^{20} - 23X^{18} + 219X^{16} - 1121X^{14} + 3356X^{12} - 5999X^{10} + 6277X^8 - 3606X^6 + 991X^4 - 95X^2 + 1 = 0$

$M_n(X) = (X^4 - 5X^2 + 3)M_{n-1}(X) - (X^4 - 3X^2 + 3)M_{n-2}(X) + M_{n-3}(X)$

$X^8 - 8X^6 + 18X^4 - 2X^3 - 12X^2 + 2X + 1 = 0$

$X^{12} - 13X^{10} + 60X^8 - 2X^7 - 122X^6 + 12X^5 + 108X^4 - 18X^3 - 33X^2 + 6X + 1 = 0$

$X^{16} - 18X^{14} + 127X^{12} - 2X^{11} - 452X^{10} + 22X^9 + 869X^8 - 82X^7 - 889X^6 + 128X^5 + 436X^4 - 78X^3 - 76X^2 + 12X + 1 = 0$

$X^{20} - 23X^{18} + 219X^{16} - 2X^{15} - 1127X^{14} + 32X^{13} + 3434X^{12} - 196X^{11} - 6373X^{10} + 590X^9 + 7111X^8 - 928X^7 - 4500X^6 + 734X^5 + 1409X^4 - 246X^3 - 155X^2 + 20X + 1 = 0$

$X^{24} - 28X^{22} + 336X^{20} - 2X^{19} - 2272X^{18} + 42X^{17} + 9578X^{16} - 360X^{15} - 26295X^{14} + 1642X^{13} + 47629X^{12} - 4356X^{11} - 56317X^{10} + 6876X^9 + 41890X^8 - 6298X^7 - 18151X^6 + 3070X^5 + 3918X^4 - 644X^3 - 288X^2 + 30X + 1 = 0$

$P_n(X) = (X^4 - 5X^2 + 4)[P_{n-1}(X) + P_{n-3}(X)] - (2X^4 - 6X^2 + 6)P_{n-2}(X) - P_{n-4}(X)$

Figure 14. Deleting an edge in the dicyclopenta-fusd polyacenes series in Figure 6 gives the above series having the same recursion equations.

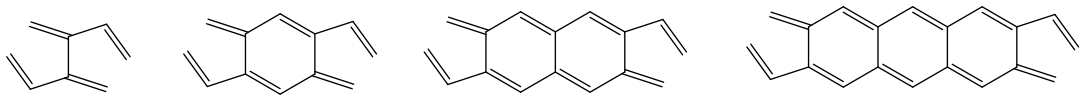

$X^8 - 7X^6 + 13X^4 - 7X^2 + 1 = 0$

$X^{12} - 12X^{10} + 50X^8 - 88X^6 + 65X^4 - 16X^2 + 1 = 0$

$X^{16} - 17X^{14} + 112X^{12} - 364X^{10} + 618X^8 - 538X^6 + 216X^4 - 30X^2 + 1 = 0$

$X^{20} - 22X^{18} + 199X^{16} - 960X^{14} + 2685X^{12} - 4446X^{10} + 4282X^8 - 2256X^6 + 568X^4 - 50X^2 + 1 = 0$

$X^{24} - 27X^{22} + 311X^{20} - 2001X^{18} + 7916X^{16} - 20000X^{14} + 32522X^{12} - 33532X^{10} + 21060X^8 - 7454X^6 + 1281X^4 - 77X^2 + 1 = 0$

$M_n(X) = (X^4 - 5X^2 + 3)M_{n-1}(X) - (X^4 - 3X^2 + 3)M_{n-2}(X) + M_{n-3}(X) + X^2$

$X^8 - 7X^6 + 13X^4 - 7X^2 + 1 = 0$

$X^{12} - 12X^{10} + 50X^8 - 90X^6 + 69X^4 - 18X^2 + 1 = 0$

$X^{16} - 17X^{14} + 112X^{12} - 368X^{10} + 646X^8 - 596X^6 + 260X^4 - 40X^2 + 1 = 0$

$X^{20} - 22X^{18} + 199X^{16} - 966X^{14} + 2757X^{12} - 4758X^{10} + 4898X^8 - 2834X^6 + 804X^4 - 80X^2 + 1 = 0$

$X^{24} - 27X^{22} + 311X^{20} - 2009X^{18} + 8052X^{16} - 20914X^{14} + 35658X^{12} - 39468X^{10} + 27312X^8 - 10936X^6 + 2169X^4 - 147X^2 + 1 = 0$

$P_n(X) = (X^4 - 5X^2 + 4)[P_{n-1}(X) + P_{n-3}(X)] - (2X^4 - 6X^2 + 6)P_{n-2}(X) - P_{n-4}(X) + 2X^2$

Figure 15. Deleting an edge in each pentagonal ring in the dicyclopenta-fusd polyacenes series in Figure 6 gives the above series. Note that the recursion equations are identical to those for the polyacene-2,x-quinododimethide series in Figure 7. Note the end terms are the same and deleting the vinyl substituents gives the same series structures.

the tail term are determined for the initial phenacene members which display a Fibonacci-like pattern ($t_n = t_{n-1} + t_{n-2}$). The characteristic equation ($X^2 - X - 1 = 0$) of this Fibonacci-like sequence gives the roots $r_1 = ½(1 + √5)$ and $r_2 = ½(1 - √5)$. Solution of $t_n = t_{n-1} + t_{n-2}$ using these roots $t_n = c_1r_1^n + c_2r_2^n$ requires input of initial conditions. For $n = 0$ one gets $15 = c_1 + c_2$ and for $n = 1$ one gets $26 = ½c_1(1 + √5) + ½c_2(1 - √5)$ Solving for c_1 and c_2 gives $c_1 = 15.77345$ and $c_2 = -0.77345$. These values give $t_n = 15.77345(1.618034)^n - 0.77345(-0.618034)^n$. Inserting $n = r - 5$ gives $t_{r-5} = 15.77345(1.618034)^{r-5} - 0.77345(-0.618034)^{r-5} = 1.422291(1.618034)^r + 8.57769(-0.618034)^r$ for $r \geq 5$. For $r = 5$ one gets $t_0 = 15.77345 - 0.77345 = 15$ and for $r = 6$ one gets $t_1 = 25.52198 + 0.47802 = 25.99999$. Note that the last term is alternating in sign and decreasing in magnitude. Thus, for $r > 6$ the last term can be ignored for simplicity as it is increasingly less significant.

The *DS* values for the linear polyacenes in Figure 17 are smaller than their phenacene isomers in Figure 18 except for anthracene (*DS* = 48) and phenanthrene (*DS* = 47).

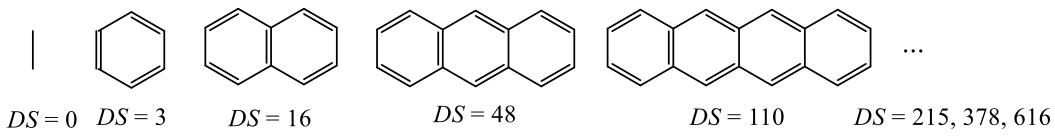

$DS[\text{acenes}] = (1/12)(r^4 + 12r^3 + 17r^2 + 6r)$ where r = No. rings = generation membership

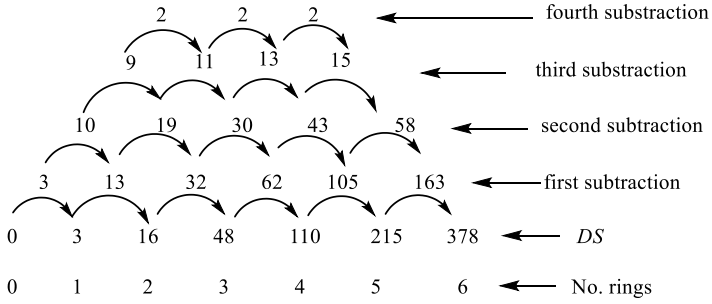

$$DS = (1/4!)(2r^4 + ar^3 + br^2 + cr + d)$$
$$= (1/4!)(2r^4 + 24r^3 + 34r^2 + 12r)$$
$$= (1/12)(r^4 + 12r^3 + 17r^2 + 6r)$$

r = No. rings

a, b, c, d are determined by matrix algebra

Figure 16. Algorithm for deriving DS analytical expressions: (1) The DS's are determined for several initial members of a series built by a given aufbau unit. (2) Successive subtraction is performed until the differences become constant. (3) The highest power term equals the number of subtraction iterations. (4) The coefficient of the highest power equals the constant difference value which also coincides with the K value of the smallest cyclic member of the series. (5) The denominator is the factorial of the highest power value. (6) Other coefficients are determined by matrix algebra.

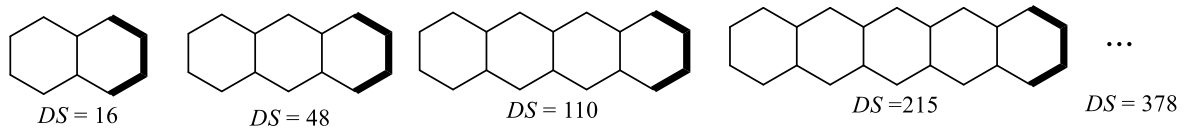

$$DS = |a_{N\text{-}2}{}^{ac}| - (N/2)\boldsymbol{K}$$

$DS_{r\text{-}3} = 9 - 3x2 = 3$
$DS_{r\text{-}2} = 31 - 5x3 = 16$
$DS_{r\text{-}1} = 76 - 7x4 = 48$
$DS_r = 155 - 9x5 = 110$

$M_{r-3}(X)$ $X^6 - 6X^4 + 9X^2 - 2 = 0$
$M_{r-2}(X)$ $X^{10} - 11X^8 + 41X^6 - 61X^4 + 31X^2 - 3 = 0$
$M_{r-1}(X)$ $X^{14} - 16X^{12} + 98X^{10} - 290X^8 + 429X^6 - 294X^4 + 76X^2 - 4 = 0$
$M_r(X)$ $X^{18} - 21X^{16} + 180X^{14} - 814X^{12} + 2096X^{10} - 3092X^8 + 2497X^6 - 993X^4 + 155X^2 - 5 = 0$

$$M_n(X) = (X^4 - 5X^2 + 3)M_{n-1}(X) - (X^4 - 3X^2 + 3)M_{n-2}(X) + M_{n-3}(X)$$
$$DS_r = 3DS_{r\text{-}1} - 3DS_{r\text{-}2} + DS_{r\text{-}3} + 2r + 3$$

$110 = 3x48 - 3x16 + 3 + ? = 99 + ? = 99 + 11$ $r = 4$ $11 = 2x4 + 3$
$215 = 3x110 - 3x48 + 16 + ? = 202 + ? = 202 + 13$ $r = 5$ $13 = 2x5 + 3$
$378 = 3x215 - 3x110 + 48 + ? = 363 + ? = 363 + 15$ $r = 6$ $15 = 2x6 + 3$

Figure 17. The recursion equation for the number of Dewar resonance structures (DS) takes the same form as the general matching polynomial recursion equation where the end term must be solved by inspection.

CONCLUSION

Several important results in this work should be noted. The recursion equations of this work demonstrate that by studying homologous series, one can extrapolate properties of larger members from the known properties of the smaller members. Per Table 1 it is evident that the homologous series in Figures 5, 6, and 14 (middle and lower) have larger TCE values than TRE values. This means that all these compounds have more conjugation energy than aromatic resonance energy. On-Surface and single molecule methods for synthesizing reactive compounds have been recently developed.[45,52] This work is a continuation of our studies toward exploiting symmetry to break up a molecule into smaller parts that are more easily solved for the eigenvalues belonging to the parent molecule.

Acknowledgment. This work was supported in part by a grant from by the UM Board of Curators (K0906077).

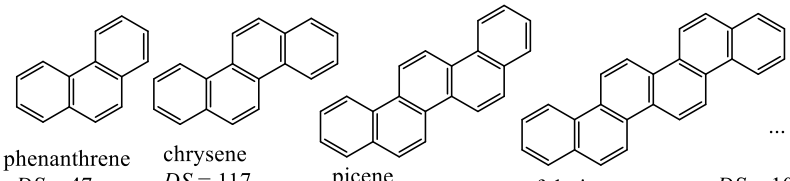

phenanthrene $DS = 47$ chrysene $DS = 117$ picene $DS = 259$ fulminene $DS = 538$ ... $DS = 1067, 2050, 3845, 7081, 12853, 23060, 40979,...$

$X^6 - 6X^4 + 9X^2 - 2 = 0$

$X^{10} - 11X^8 + 41X^6 - 61X^4 + 31X^2 - 3 = 0$

$X^{14} - 16X^{12} + 98X^{10} - 291X^8 + 435X^6 - 305X^4 + 82X^2 - 5 = 0$

$X^{18} - 21X^{16} + 180X^{14} - 816X^{12} + 2117X^{10} - 3173X^8 + 2638X^6 - 1102X^4 + 189X^2 - 8 = 0$

$DS = |a_{N-2}{}^{ac}| - (N/2)\boldsymbol{K}$

$DS_{r-3} = 9 - 2x3 = 3$

$DS_{r-2} = 31 - 3x5 = 16$

$DS_{r-1} = 82 - 5x7 = 47$

$DS_r = 189 - 8x9 = 117$

$M_n(X) = (X^4 - 5X^2 + 3)M_{n-1}(X) - (X^4 - 2X^2 + 2)M_{n-2}(X) - (X^4 - 3X^2 + 1)M_{n-3}(X) + M_{n-4}(X)$

$DS_r = 3DS_{r-1} - 2DS_{r-2} - DS_{r-3} + DS_{r-4} + 1.4223(1.618034)^r$; $\boldsymbol{K}_r = 1.17082(1.618034)^r$; $r > 5$

$259 = 3x117 - 2x47 - 16 + 3 + ? = 244 + ?$ $\quad 259 - 244 = 15 \quad t_{n-2}$

$538 = 3x259 - 2x117 - 47 + 16 + ? = 512 + ?$ $\quad 538 - 512 = 26 \quad t_{n-1}$

$1067 = 3x538 - 2x259 - 117 + 47 + ? = 1026 + ?$ $\quad 1067 - 1026 = 41 \quad t_n$

} Fibonacci-like sequence

$t_n = t_{n-1} + t_{n-2}$; $t_n - t_{n-1} - t_{n-2} = 0$; $t_0 = 15$ and $t_1 = 26$ for $n = 2$

$t_n - t_{n-1} - t_{n-2} = 0$ gives the characteristic equation of $X^2 - X - 1 = 0$ with roots $r_1 = \frac{1}{2}(1 + \sqrt{5})$ and $r_2 = \frac{1}{2}(1 - \sqrt{5})$

Therefore $t_n = c_1 r_1{}^n + c_2 r_2{}^n$ and for $n = 0$ one gets $15 = c_1 + c_2$ and for $n = 1$ one gets $26 = c_1\frac{1}{2}(1 + \sqrt{5}) + c_2\frac{1}{2}(1 - \sqrt{5}) = 1.618034c_1 - 0.618034c_2 = 1.618034c_1 - 0.618034(15 - c_1) = 2.236068c_1 - 9.2751$ which gives after rearranging $35.27051 = 2.236068c_1$; thus $c_1 = 15.77345$ and $c_2 = -0.77345$.

$t_n = 15.77345(1.618034)^n - 0.77345(-0.618034)^n = 15.77345(1.618034)^{r-5} - 0.77345(-0.618034)^{r-5}$ because $n = r - 5$.

This gives $t_{r-5} = 1.422291(1.618034)^r + 8.57769(-0.618034)^r$ for $r \geq 5$; for $r = 5$ one gets $t_0 = 15.77345 - 0.77345 = 15$ and for $r = 6$ one gets $t_1 = 25.52198 + 0.47802 = 25.99999$. Note that the last term is alternating in sign and decreasing in magnitude. Thus, for $r > 6$ the last term can be ignored for simplicity as it is increasingly less significant.

Figure 18. From the general matching polynomial recursion equation, one can get the recursion equation for the number of Dewar resonance structures (DS) where the end term must be solved by inspection. The above residue end term is related to a Fibonacci-like sequence.

REFERENCES

[1] J. A Aihara, *J. Am. Chem. Soc.* **1976**, *98*, 2750–2758. https://doi.org/10.1021/ja00426a013

[2] I. Gutman, M. Milun, N. Trinajstić, *J. Am. Chem. Soc.* **1977**, *99*, 1692–1704. https://doi.org/10.1021/ja00448a002

[3] J. R. Dias, *J. Phys. Chem. A* **2011**, *115*, 13619–13627. https://doi.org/10.1021/jp207531u

[4] J. R. Dias, *J. Phys. Chem. A* **2013**,*117*, 4716–4725. https://doi.org/10.1021/jp403380t

[5] J. R. Dias, *Molec. Phys.* **2015**, *113*, 3389–3394. https://doi.org/10.1080/00268976.2015.1025882

[6] J. Aihara, *Bull. Chem. Soc., Jpn.* **2016**, *89*, 1425–1454. https://doi.org/10.1246/bcsj.20160237

[7] J. Aihara, *J. Phys. Chem. A* **1999**, *103*, 7487–7495. https://doi.org/10.1021/jp990092i

[8] J. R. Dias, *J. Chem. Inf. Model.* **2005**, *45*, 562–571. https://doi.org/10.1021/ci0500334

[9] M. D. Wodrich, C. S. Wannere, Y. Mo, P. D. Jarowski, K. N. Houk, P. von R. Schleyer, *Chem. Eur. J.* **2007**, *13*, 7731–7744. https://doi.org/10.1002/chem.200700602

[10] D. J. Klein, M. Randic, *J. Comput. Chem.* **1987**, *8*, 516–521. https://doi.org/10.1002/jcc.540080432

[11] M. Bendikov, H. M. Dulong, K. Starkey, K. N. Houk, E. A. Carter, F. Wudl, *J. Am. Chem. Soc.* **2004**, *126*, 7416–7417. https://doi.org/10.1021/ja048919w

[12] J. Aihara, H. Kanno, *J. Phys. Chem. A* **2005**, *109*, 3717–3721. https://doi.org/10.1021/jp047183m

[13] T. Ishida, J. Aihara, *Phys. Chem. Chem. Phys.* **2009**, *11*, 7197–7201. https://doi.org/10.1039/b903815a

[14] M. Das, *J. Chem. Phys.* **2015**, *143*, 064704-1 to 064704-19. https://doi.org/10.1063/1.4928571

[15] C. Ibeji, D. Ghosh, *Phys. Chem. Chem. Phys.* **2015**, *17*, 9849–9856. https://doi.org/10.1039/C5CP00214A

[16] F. Senn, M. Krykunov, *J. Phys. Chem. A* **2015**, 10575–10581. https://doi.org/10.1021/acs.jpca.5b07075

[17] K. Bhaskaran-Nair, K. Kowalski, M. Jarrell, J. Moreno, *Chem. Phys. Lett.* **2015**, *641*, 146–152. https://doi.org/10.1016/j.cplett.2015.10.071

[18] K. B. Wiberg, *J. Org. Chem.* **1997**, *62*, 5720–5727. https://doi.org/10.1021/jo961831j

[19] M. K. Cyranski. B. T. Stepien, T. M. Krygowski, *Tetrahedron* **2000**, *56*, 9663–9667. https://doi.org/10.1016/S0040-4020(00)00919-4

[20] G. Portella, J. Poster, J. M. Bofill, P. Alemany, M. Solá, *J. Org. Chem.* **2005**, *70*, 2509–2521. https://doi.org/10.1021/jo0480388
[21] J. R. Dias, *Croat. Chem. Acta* **2013**, *86*, 379–386. https://doi.org/10.5562/cca2292
[22] H. Hosoya, M. Aida, R. Kumagal, K. Watanabe, *J. Comput. Chem.* **1987**, *8*, 358–386. https://doi.org/10.1002/jcc.540080412
[23] H.Hosoya, H.Kumazaki, K. Chida, M.Ohuchi, Y.-D. Gao, *Pure & Appl. Chem.* **1990**, *62*, 445–450. https://doi.org/10.1351/pac199062030445
[24] J. Aihara, *J. Chem. Soc. Perkin Trans. 2* **1994**, 971–974. https://doi.org/10.1039/p29940000971
[25] K. N. Houk, P. S. Lee, M. Nendel, *J. Org. Chem.* **2001**, *66*, 5517–5521. https://doi.org/10.1021/jo010391f
[26] R. Rieger, K. Müllen, *J. Phys. Org. Chem.* **2010**, *23*, 315–325. https://doi.org/10.1002/poc.1644
[27] J. Aihara, M. Makino, *Chem. Asian J.* **2008**, *3*, 585–591. https://doi.org/10.1002/asia.200700287
[28] J. R. Dias, *J. Phys. Chem. A* **2014**, *118*, 10822–10836. https://doi.org/10.1021/jp5083906
[29] M. Makino, J. Aihara, *Phys. Chem. Chem. Phys.* **2008**, *10*, 591–599. https://doi.org/10.1039/B714906A
[30] K. Balasubramanian, *J. Comput. Chem.* **1984**, *5*, 387–394. https://doi.org/10.1002/jcc.540050417
[31] R. Ramaraj, K. Balasubramanian, *J. Comput. Chem.* **1985**, *6*, 122–141. https://doi.org/10.1002/jcc.540060207
[32] R. B. Mallion, D. H. Rouvray, *J. Mat. Chem.* **1990**, *5*, 1–21. https://doi.org/10.1007/BF01166272
[33] J. R. Dias, *J. Molec. Struct. (THEOCHEM)* **1988**, *165*, 125–148. https://doi.org/10.1016/0166-1280(88)87011-8
[34] J. R. Dias, *Int. J. Chem. Model.* **2013**, *5*, 167–181.
[35] J. R. Dias, *Theor. Chim. Acta* **1985**, *68*, 107–123. https://doi.org/10.1007/BF00527527
[36] H. Hosoya, N. Ohkami, *J. Comput. Chem.* **1983**, *4*, 585–593. https://doi.org/10.1002/jcc.540040418
[37] T. Yamaguchi, M. Suzuki, H. Hosoya, *Nat. Sci. Report, Ochanomizu Univ.* **1975**, *26*, 39–60.
[38] H. Hosoya, A. Uchiyama, M. Kadota, K. Chida, M. Aida, T. Yamaguchi, *Nat. Sci. Report, Ochanomizu Univ.* **1986**, *37*, 133–168.
[39] J. R. Dias, *Molec. Phys.* **2010**, *108*, 3425–3429. https://doi.org/10.1080/00268976.2010.518980
[40] J. R. Dias, *J. Phys. Chem. A* **1997**, *101*, 7167–7175. https://doi.org/10.1021/jp971552f
[41] J. R. Dias, *Molec. Phys.* **2013**, *111*, 735–751. https://doi.org/10.1080/00268976.2012.742584
[42] Z. Chen, D. Jiang, X. Lu, H. F. Bettinger, S. Dai, P. Von R. Schleyer, K. N. Houk, *Org. Lett.* **2007**, *9*, 5449–5452. https://doi.org/10.1021/ol7023339
[43] S. Radenkovic, S. Markovic, R. Kuc, N. Stankovic, *Montatsh. Chem.* **2011**, *142*, 1013–1019. https://doi.org/10.1007/s00706-011-0557-8
[44] A. Jancarik, J. Holec, Y. Nagata, M. Samal, A. Gourdon, *ChemRxiv* **2021**, 1–13. https://doi.org/10.1038/s41467-021-27809-0
[45] R. Zuzak, R. Dorel, M. Kolmer, M. Szymonski, S. Godlewski, A. M. Echavarren, *Angew. Chem. Int. Ed.* **2018**, *57*, 10500–10505. https://doi.org/10.1002/anie.201802040
[46] T. Bally, S. Chai, M. Neuenschwander, Z. Zhu, *J. Am. Chem. Soc.* **1997**, *119*, 1869–1875. https://doi.org/10.1021/ja963439t
[47] R. W. A. Havenith, J. J. Engelberts, P. W. Fowler, E. Steiner, J. H. van Lenthe, P. Lazzeretti, *Phys. Chem. Chem. Phys.* **2004**, *6*, 289–294. https://doi.org/10.1039/B311255A
[48] I. G. Cuesta, S. Coriani, P. Lazzeretti, A. M. J. S. de Meras, *ChemPhysChem.* **2006**, *7*, 240–244. https://doi.org/10.1002/cphc.200500327
[49] J. R. Dias, *Chem. Phys. Lett.* **2016**, *647*, 79–84. https://doi.org/10.1016/j.cplett.2016.01.055
[50] J. R. Dias, *J. Phys. Chem. A* **2016**, *120*, 3975–3982. https://doi.org/10.1021/acs.jpca.6b03897
[51] H. Okamoto, S. Hamao, R. Eguchi, H. Goto, Y. Takabayashi, P. Y.-H. Yen, L. U. Liang, C.-W. Chou, G. Hoffmann, S. Gohda, H. Sugino, Y.-F. Liao, H. Hirofumi Ishii, Y. Kubozono, *Sci. Rep.* **2019**, *9*, 2045–2322. https://doi.org/10.1038/s41598-019-39899-4
[52] J. R. Dias, *ACS Omega* **2023**, *8*, 18332–18338. https://doi.org/10.1021/acsomega.3c02488